International Journal of Neural Systems, Vol. 27, No. 7 (2017) 1750022 (17 pages)

DOI: 10.1142/S0129065717500228

Online Automated Seizure Detection in Temporal Lobe Epilepsy Patients Using Single-lead ECG

Thomas De Cooman*, Carolina Varon and Borbála Hunyadi
Department of Electrical Engineering
KU Leuven, Kasteelpark Arenberg 10, Box 2446
Leuven, 3000, Belgium
imec, Leuven, Belgium
**thomas.decooman@esat.kuleuven.be*

Wim Van Paesschen
Department of Neurology
UZ Leuven and KU Leuven, Herestraat 49
Leuven, 3000, Belgium

Lieven Lagae
Department of Child Neurology
UZ Leuven and KU Leuven, Herestraat 49
Leuven, 3000, Belgium

Sabine Van Huffel
Department of Electrical Engineering
KU Leuven, Kasteelpark Arenberg 10 box 2446
Leuven, 3000, Belgium
imec, Leuven, Belgium

Accepted 8 February 2017
Published Online 31 March 2017

Automated seizure detection in a home environment has been of increased interest the last couple of decades. The electrocardiogram is one of the signals that is suited for this application. In this paper, a new method is described that classifies different heart rate characteristics in order to detect seizures from temporal lobe epilepsy patients. The used support vector machine classifier is trained on data from other patients, so that the algorithm can be used directly from the start of each new recording. The algorithm was tested on a dataset of more than 918 h of data coming from 17 patients containing 127 complex partial and generalized partial seizures. The algorithm was able to detect 81.89% of the seizures, with on average 1.97 false alarms per hour. These results show a strong drop in the number of false alarms of more than 50% compared to other heart rate-based patient-independent algorithms from the literature, at the expense of a slightly higher detection delay of 17.8s on average.

Keywords: Epilepsy; electrocardiogram; seizure detection; home monitoring.

1. Introduction

Epilepsy is a neurological disorder that affects around 1% of the people worldwide.[1] In around 30–40% of the cases, epilepsy cannot be cured with anti-epileptic drugs. To improve the quality of life of these refractory epilepsy patients at home, several solutions are possible. One of these solutions is the use of an alarm system in which the seizures are detected automatically. Relatives and friends of the patient can then be warned so that they can come

and help the patient when a seizure occurs. Another solution would be to use automated seizure detection in a closed-loop system with vagus nerve stimulation (VNS).[2] VNS can then be activated if a seizure is detected, thereby shortening the seizure duration.[3]

Automated epileptic seizure detection is typically done by analysis of the electroencephalogram (EEG). Obtaining EEG is however very impracticable outside the hospital.[4] Previous studies showed that other easily acquired signals such as the electrocardiogram (ECG), accelerometry, electromyogram and electrical dermal activity can also be used to detect certain types of seizures in an automated fashion.[5] In this paper, single-lead ECG is used to detect complex partial and secondary generalized seizures in temporal lobe epilepsy (TLE).

Seizures from TLE patients are often accompanied with a strong ictal heart rate increase (HRI).[6–8] These HRIs often follow a pattern (see Fig. 1 for the most common ictal pattern), in which the heart rate (HR) first increases linearly, then stays stable at a certain peak heart rate, and finally decreases exponentially.[8,9] Variations on this ictal HR behavior can however occur as well.[10] Despite the strong patient-dependency of HR features, the patient-independent approach is preferred for online seizure detection in practice. This is mainly due to two drawbacks of patient-specific seizure detection:

- There should be sufficient (seizure) data available of the specific patient before the algorithm can be used. This could take more than a week for some patients (for patients with a low seizure frequency), which would be a problem for short-term applications. In this case, data collected during diagnostic monitoring will not be sufficient in order to make a robust patient-specific algorithm.
- The data of every new tested patient should be correctly annotated. This is typically done using the gold standard (video-EEG monitoring), and requires the cooperation of medical experts for accurate results.

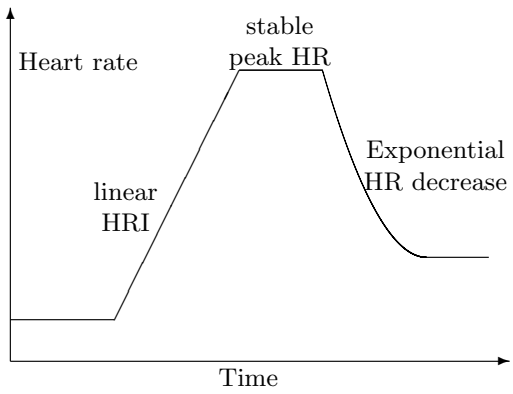

Fig. 1. Illustration of ictal heart rate changes during temporal lobe seizures.

State-of-the-art HR-based seizure detection algorithms are all based on thresholding approaches. Most of them, however, do not recommend parameter settings for patient-independent use.[9–11] Ungureanu *et al.*[12] uses minimal patient-specific prior information (the patient's age) in order to tune these parameters to that patient, which is still acceptable for the intended patient-independent goal. In this paper, the algorithm is trained automatically in order to optimize seizure detection parameters by using support vector machines (SVM).

Most of the algorithms in the literature try to detect the seizures as fast as possible, already a couple of seconds after the seizure onset. Studies however show that the entire HRI might contain important information (such as the peak HR) for automated seizure detection.[13,14] Therefore, a method is proposed that analyzes the entire HRI. Features of HRIs are then extracted and classified using a patient-independent SVM classifier — using leave-one-patient-out crosstesting (LOPO CT)— into seizure and nonseizure HRIs. Although machine learning has been discussed in previous works for offline seizure detection in neonates,[15,16] it has not been thoroughly investigated for online HR-based seizure detection in adults and children.

Different algorithms from the literature will be implemented and tested on the same dataset as the proposed algorithm. To our knowledge, this is the first time multiple HR-based seizure detection algorithms are evaluated on the same dataset.

The used dataset is summarized in Sec. 2. The proposed patient-independent seizure detection algorithm is described in Sec. 3. The results of the proposed algorithm and the implementations of several algorithms from the literature are shown and

Table 1. Overview of the used dataset.

Patient number	Patient age	Number of seizures	Seizure types[a]	Record duration[b]
1	37	4	1	23:20:19
2	49	10	2,3	26:30:50
3	41	9	2	63:03:34
4	27	13	1,2	70:59:30
5	35	5	2	53:04:57
6	15	10	3	24:40:45
7	17	4	2	43:02:34
8	29	11	2,3	47:06:33
9	27	4	2	30:38:16
10	33	1	1	02:06:25
11	54	2	1,2	15:06:09
12	26	7	1,2	148:08:27
13	34	2	2	10:59:55
14	52	3	1,2	45:37:02
15	9	30	2,3	66:57:00
16	38	11	1,2,3	113:47:48
17	46	1	2	133:12:28
Total	[9–54]	127	—	918:10:04

Notes: [a]indicates the seizure severity classes found for each patient (see Sec. 4.8).
[b]Record duration expressed in hh:mm:ss.

discussed in Sec. 4. A precursor of this paper has been discussed in Ref. 17.

2. Data Acquisition

The proposed algorithm was developed based on a dataset containing single-lead ECG recordings from 18 patients with refractory TLE, who underwent presurgical evaluation at UZ Leuven. All patients gave consent to their participation in this study. Patients were allowed to move freely inside their hospital room during monitoring. Analysis of one of these patients was left out from this study due to poor overall ECG quality. Seizure onsets were annotated by a clinical expert using video-EEG monitoring as part of a presurgical evaluation, independently of this study. In total 127 complex partial and secondary generalized seizures were recorded during more than 918 h of continuous ECG data. Table 1 gives a detailed overview of this dataset. The ECG was recorded from lead II with a sampling frequency of 250 Hz.

3. Methodology

The online seizure detection algorithm using heart rate consists of three main stages: significant HRI extraction, feature extraction and seizure detection. The different steps are shown in Fig. 2 and are discussed in this section.

3.1. *Online R peak detection*

In a first step, the single-lead ECG is processed in order to obtain the immediate HR measurements. The immediate HR is computed as

$$\mathrm{HR} = \frac{60}{\mathrm{RR}}, \tag{1}$$

with RR the time difference between consecutive R peaks in seconds. The tachogram is defined as the time series of these instantaneous heart rates. The automated online detection of the R peaks is done by using an adapted version of the R peak detection algorithm described in Ref. 18. The algorithm is adapted in order to operate online according to the following steps:

(1) The ECG is filtered by a low-pass (cut-off frequency 40Hz) and a high-pass (5Hz) Butterworth filter.
(2) The derivative of this signal is computed.

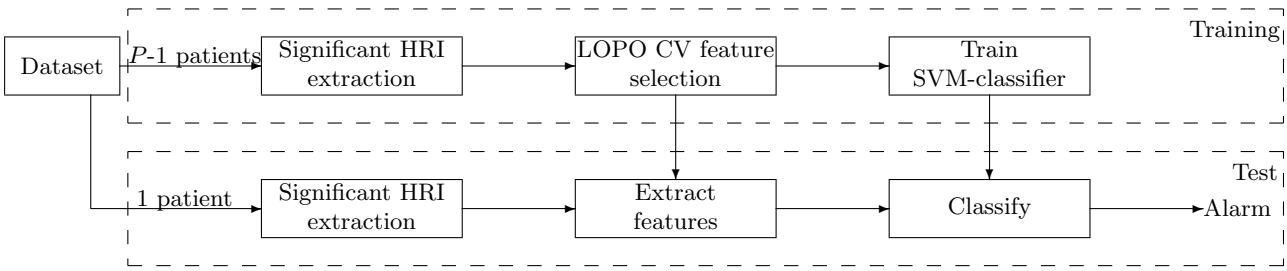

Fig. 2. Overview of the followed procedure for P patients in the dataset ($P = 17$ here). For every tested patient, feature selection and classifier training are performed on all other patients in the available dataset. This procedure is then repeated for every patient. The significant HRI extraction procedure is identical for all patients.

(3) Positive maximum peaks P^+ above a threshold $\frac{T^+}{1.5}$ and a negative minimum peak P^- below a threshold $\frac{T^-}{1.5}$ are searched in real time. If a combination of such a P^+ and P^- are found with a peak-to-peak distance lower than 140ms, an R peak is detected.

(4) T^+ is updated online as

$$T^+ = 0.8 * T^+ + 0.2 * P^+ \tag{2}$$

and similarly for T^- with P^-.

The different fixed factors in this algorithm were chosen after analysis of their performance on the MIT-BIH arrythmia database.[19,20] T^+ and T^- are initialized as the positive/negative peak values from the third largest/smallest maximum/minimum in the first 5 s from the recording. The online search-back procedure from Ref. 21 was also added to this procedure for improved R peak detection performance.

3.2. *Extraction of significant HRI*

The ictal HR changes should now be detected automatically from the online constructed heart rate signal. Detecting the complete ictal HR pattern as shown in Fig. 1 however has some important drawbacks. First, the entire ictal HR pattern can take over 2 min in some cases, which would lead to a too large detection delay for early seizure detection. A second issue is the fact that multiple variants of the shown ictal pattern exist in practice.[10,22] Therefore, this paper restricts itself to detecting and analyzing the incremental phase of the ictal HR pattern. It allows a faster detection of the seizures, and contains sufficient information for accurate seizure detection.[9,10,12,17,23]

The proposed preprocessing algorithm (called *HRI-EXTRACT* from now on) detects this linear HRI phase in three stages, which are mainly based on using the gradient of the tachogram. The tachogram is first filtered by applying a median filter (with a filter order of 15 HR measurements). This is done in order to remove smaller peaks inside the linear phase due to respiratory sinus arrhythmia or R peak detection errors. This improves the robustness of the significant HRI extraction procedure. The gradient ∇HR is computed as the gradient of the linear fit on 10 HR measurements. In a first stage, the algorithm looks for a gradient larger than 1bpm/s. If such a gradient is found, the algorithm assumes that a strong HRI is occurring. In the second stage, the algorithm searches back in time for when this HRI started (t_{start}). This is done by searching for the last point for which the gradient is negative or near zero. In the third stage, the end of the linear phase (t_{end}) is found by again searching for the first negative gradient.

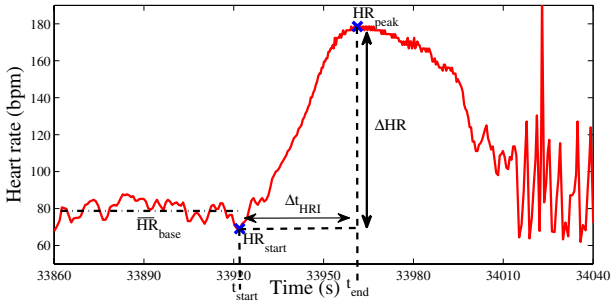

Fig. 3. Example of an ictal HRI from patient 17. The features required for the extraction of significant HRIs are defined in this figure. $\overline{\text{HR}}_{\text{base}}$ indicates the average HR over the 60s before the start of the HRI. HR_{start} indicates the HR at the beginning of the HRI, HR_{peak} the peak HR at the end of the HRI. Δt_{HRI} indicates the length of the HRI (in seconds), ΔHR indicates the amount of increased HR. The EEG seizure onset is located at 33,922s in this example.

Once the end of the HRI is found (at time t_{end}), several heart rate features are extracted from this HRI phase, and the following rules are imposed (see Fig. 3 for the definition of different variables):

$$\Delta\text{HR} > 10\text{bpm}, \tag{3a}$$

$$\frac{\text{HR}_{\text{peak}}}{\overline{\text{HR}}_{\text{base}}} > 1.1, \tag{3b}$$

$$\frac{\text{HR}_{\text{peak}}}{\text{HR}_{\text{rest}}} > 1.25, \tag{3c}$$

$$\frac{\Delta\text{HR}}{\Delta t_{\text{HRI}}} > 0.35\text{bpm/s}. \tag{3d}$$

HR_{rest} stands for the estimated average HR at rest for the patient under testing and is computed on-the-run. HR_{rest} is set to $\overline{\text{HR}}_{\text{base}}$ if

- $\overline{\text{HR}}_{\text{base}} < \text{HR}_{\text{rest}}$,
- the linear fit on the data of HR_{base} results in an absolute gradient < 0.2bpm/s and
- the linear fit is found with $R^2 > 0.7$.

These rules were set after analyzing a different dataset in Ref. 17. As this step is used as a preprocessing step, rule values were chosen so that all seizure HRIs were detected in that database. If the HRI follows the rules from Eqs. (3a)–(3d), it is assumed that it is a significant HRI, and further processing is required. This algorithm is completely identical for all patients and is summarized in Algorithm 1.

Algorithm 1 *HRI-EXTRACT*

Input: Online HR data
Output: Information of a significantly strong HRI
for each new HR measurement HR_k at time t_{HR_k} **do**
  Filter HR data using median filter
  Compute HR gradient ∇HR_k
  if not currently looking for end of a HRI
    if $\nabla HR_k > 1 bpm/s$
      Look back for last $\Delta HR \leq 0 bpm/s$: start of HRI t_{start}
      Start looking online for t_{end}
    end if
  else if $\nabla HR_k \leq 0 bpm/s$
    Current time is end of HRI $t_{end} = t_{HR_k}$
    if Eq. 3a-3d apply
      Significant HRI detected!
    end if
    Stop looking for end of HRI
  end if
  Check if HR_{rest} needs an update
end for

3.3. *Feature extraction*

If a significant HRI is detected, several HR features are extracted from the segments before and during this HRI. The extracted features can be divided into three big groups.

The first group contains some specific HR features related to the mentioned HRI. These are amongst others $\mathrm{HR_{peak}}$, Δt_{HRI} and the maximal HR gradient $\nabla \mathrm{HR_{max}}$ during the HRI, which were also discussed in Sec. 3.2. The second group contains several heart rate variability (HRV) features extracted from the HRI period. These include linear HRV statistics like the standard deviation of successive differences (SDSD) conform the Task Force recommendations.[24] The last group of features consists of linear HRV features and several HR frequency features extracted from the 60s preceding the HRI.

3.4. *Feature selection*

In the last phase of the algorithm, the features of significant HRI's are classified in order to indicate if these are caused by an epileptic seizure or not. As mentioned in Sec. 1, a patient-independent classifier is preferred here. The classifier is trained on data from other patients than the tested patient (LOPO CT) as illustrated in Fig. 2. The feature selection is also done for each patient separately, using only the data from other patients.

In this paper, forward feature selection is used, incrementally adding features to the pool of selected features. The first two features are added simultaneously as a lot of HR features are strongly correlated to each other. Let S be the collection of selected features (initially empty) and the set of N_f features $X = [X^1, \ldots, X^{N_f}]$. The first two selected features are then

$$S^1 = \{[X^{k'}, X^{l'}]\} \tag{4}$$

with

$$[k', l'] = \underset{k,l|k\neq l}{\arg\max} F_\beta(\mathrm{SVM}([X^k, X^l])) \quad k, l = 1, \ldots, N_f \tag{5}$$

and

$$F_\beta = (1+\beta^2) * \frac{\mathrm{Se} * \mathrm{PPV}}{(\beta^2 * \mathrm{Se}) + \mathrm{PPV}} \tag{6}$$

the F_β-score, in which Se stands for the sensitivity and PPV stands for the positive predictive value of the SVM classifier outputs using the selected features $[X^k, X^l]$. The β parameter allows to give β times more importance to sensitivity than to PPV in the computation of the F-score. Additional features were added to S iteratively as

$$S^{m+1} = \{S^m \cup X^{j'}\}, \quad m \geq 2 \tag{7}$$

with

$$j' = \underset{j\notin S^m}{\arg\max} F_\beta(\mathrm{SVM}(S^m \cup X^j)), \quad j = 1, \ldots, N_f \tag{8}$$

as long as the addition of this feature $X^{j'}$ leads to an increased F_β-score on the validation set.

Table 2. Comparison of F_β results for different typical heart rate-based seizure detection results during training. All F_β-scores, PPV and sensitivity (Se) are shown in percentages.

Based on	Se	FP/h	PPV	F_1	F_3	F_5
F_1	74.6	1.9	5.1	9.6	31.6	49.0
F_3	74.6	1.9	5.1	9.6	31.6	49.0
F_5	82.5	2.2	4.8	9.1	31.5	50.9

The SVM output is found by using LOPO cross-validation (LOPO CV) on the training set (see next section for classifier details). This means that the training set is split up so that the classifier is trained on every patient with exception of one patient, which is the patient used for validation. The trained classifier is then evaluated on this patient in the validation set. This procedure is then repeated so that every patient in the training set is used once for validation. The output for the different validation datesets are then combined to one general sensitivity and PPV output value for the training set. To lower the unbalance in the training sets, the nonseizure samples were limited to the first 100 nonseizure samples of each patient during the training step, similarly as in Ref. 25.

Table 2 gives an example of the F_β-scores for different β values during feature selection. The F_5-score leads to the extraction of features that result in a more desirable sensitivity (around 80%) and an acceptable false alarm rate (±2FPs/h) compared to lower β values. Therefore, the F_5-score is used in this paper.

This method of feature selection is chosen here as it is able to identify features that work well in the used generic way. Features that lead to a good classification result in patients for which no data was used during training were chosen, so that the patient-specific impact on the feature selection is reduced as much as possible.

3.5. *Classification*

Let $\{x_i,y_i\}$ be the training data with $x_i \in \mathbb{R}^d$ the input vector containing the selected feature data, and $y_i \in \{-1,+1\}$ the corresponding output values. Let class -1 correspond to nonseizure samples and class $+1$ to seizure samples. SVM will then map these input data to a higher dimensional space using a function $\varphi(.)$.[26] A nonlinear mapping φ then makes it possible to make a nonlinear separating hyperplane $w^T\varphi(x)+b=0$, with $w \in \mathbb{R}^d$ the unknown weight vector and $b \in \mathbb{R}$ an unknown constant. The classifier output is then defined as

$$f(x) = \text{sign}(w^T\varphi(x)+b). \tag{9}$$

The unknown variables w and b can be found by solving the following optimization problem:

$$\min_{w,b,\xi} \frac{1}{2}w^T w + C^+ \sum_{i=1|y_i=+1}^{N} \xi_i + C^- \sum_{i=1|y_i=-1}^{N} \xi_i \tag{10}$$

such that

$$y_i(w^T\varphi(x_i)+b) \geq 1-\xi_i, \quad \xi_i \geq 1, \quad i=1,\ldots,N. \tag{11}$$

Due to the unbalance in the dataset between the datapoints belonging to both classes, a modification of the typical SVM is used.[27] The values of C^+ and C^- are set here to

$$C^+ = \alpha * \frac{(N^+ + N^-)}{2 * N^+}, \tag{12}$$

$$C^- = \frac{N^+ + N^-}{2 * N^-} \tag{13}$$

with N^+ and N^- indicating the number of datapoints belonging to classes $+1$ and -1, respectively. The factor α in C^+ is added in order to increase the impact of misdetecting seizure samples compared to nonseizure samples. α is set initially to a heuristic value of 3 for the feature selection. Once the features are chosen this way, α is optimized on the training set by retraining the model for different $\alpha \in [2,5]$. The α value leading to the highest F_5-score on the training set is used for training the final SVM model. A Gaussian kernel is used in this paper. The entire procedure for seizure detection (called *HRI-SVM*) is summarized in Algorithm 2.

Algorithm 2 Procedure for online seizure detection (*HRI-SVM*)

Input: Online HR data of patient P_p, offline HRI data of other patients $pat_{pool} \backslash P_p$
Output: Alarm in case of an assumed seizure for patient P_p

Algorithm 2 (*Continued*)

Offline Preprocessing: feature selection

Let pat_{pool} be the collection of patients
Let $feat_{pool}$ be the collection of features
Initialize $feat_{sel}$ as empty and $F_5^{prev} = 0$
while adding features to $feat_{sel}$ leads to improved performance in patients $pat_{pool} \backslash P_p$ **do**
  for each feature $feat_f \in feat_{pool} \backslash \{feat_{sel}\}$ **do**
    $feat_{test} = feat_{sel} \cup feat_f$
    for each patient $P_i \in pat_{pool} \backslash \{P_p\}$ **do**
      Train classifier on HRIs of patients $pat_{pool} \backslash \{P_p, P_i\}$ using features $feat_{test}$ with α=3
      Test classifier on HRIs of patient P_i
    end for
    Evaluate F_5-score F_5^f on patients in $pat_{pool} \backslash \{P_p\}$
  end for
  if $max(F_5^f) > F_5^{prev}$
    $feat_{sel} = feat_{sel} \cup feat_{\arg\max_f F_5^f}$
    $F_5^{prev} = max(F_5^f)$
  end if
end while

Offline Preprocessing: α optimization

$alpha_{max} = 3$
for $\alpha_c \in [2, 5]$ **do**
  for each patient $P_i \in pat_{pool} \backslash \{P_p\}$ **do**
    Train classifier on HRIs of patients $pat_{pool} \backslash \{P_p, P_i\}$ using features $feat_{sel}$ with
$\alpha = \alpha_c$
    Test classifier on HRIs of patient P_i
  end for
  Evaluate F_5-score F_5^a on patients in $pat_{pool} \backslash \{P_p\}$
  if $max(F_5^a) > F_5^{prev}$
    $F_5^{prev} = max(F_5^a)$
    $\alpha_{max} = \alpha_c$
  end if
end for
Train final classifier using $feat_{sel}$ on data of $pat_{pool} \backslash P_p$ with $\alpha = \alpha_{max}$

Online Analysis of HR data from patient P_p

for each new HR measurement HR_k at time t_{HR_k} **do**
  Extract significant HRIs (see Alg. 1)
  if the end of a significant HRI is detected
    Extract selected features from the significant HRI
    Classify using patient-independent classifier with $feat_{sel}$
    if class output of classifier = 1
      Alarm!
    end if
  end if
end for

3.6. *Evaluation criteria*

Online automated seizure detection algorithms are typically analyzed using four metrics. The sensitivity gives the percentage of seizures that are detected by the algorithm. The number of false alarms are evaluated by both the number of false positives per hour (FP/h) and the PPV. The fourth metric is the detection delay, which is the delay between the seizure onset and the moment the seizure is detected by the algorithm. The seizure onset is taken as the scalp EEG onset if this is available. In some cases (for patients 2, 6 and 8), no clear EEG onsets were found. For these cases the clinical onsets are used as reference onset. Seizures were detected correctly when an alarm was given between 30s before and 90s after the seizure onset. These boundaries are chosen as none of the seizures showed any significant HRIs before 30s prior to the EEG onset, which is in consensus with the results of Ref. 28. HRIs typically end before 90s after the EEG onset, and detecting a seizure 1.5 min after the EEG onset is considered to be too late for online seizure detection. Alarms within 1 min of each other are counted as one alarm.[10] General measurements of the entire dataset can be divided into overall performance (computed on the total number of seizures) and patient-averaged performance (the average of the performances of each patient). Unless specifically mentioned, overall performance is meant for the evaluation of the general performance in the rest of the paper.

3.7. *Tested HR-based seizure detectors from the literature*

Other patient-independent seizure detection algorithms from the literature were also implemented and tested on the used dataset.[9,10,12] Also an adapted version of the mentioned algorithm, using a linear SVM with the features found in Ref. 17 ($\nabla \mathrm{HR}_{max}$, Δt_{HRI} in #RR intervals and the pre-ictal spectral entropy) is evaluated. The parameters for the algorithms from Refs. 10 and 9 (from now on referred to as *Osorio* and *vanElmpt*, respectively) are set twice so that they result in either a similar sensitivity (marked by (se)) or similar FP/h rate (marked by (fph)) as the proposed algorithm. This allows a better comparison between these algorithms and the

proposed algorithm. This procedure is not required for the algorithm from Ref. 12 as the optimal patient-independent parameter settings were already discussed in the corresponding paper. The algorithms were faithfully replicated based on the algorithm descriptions from the corresponding papers and were intensively tested for their correctness. The same R peak detection algorithm is however used for all algorithms.

4. Results and Discussion

4.1. *HRI-Extract*

The *HRI-EXTRACT* algorithm detected 116 of the 127 seizures. Some seizures were missed here either due to the absence of a strong ictal HRI or due to the presence of artifacts in the ECG during the ictal period. The nonseizure HRIs that were detected (at average 6.0 nonseizure HRIs per hour), were typically other sympathetic activations caused by nonseizure stimuli like arousals, or false detections due to R peak detection errors caused by strong ECG noise. This preprocessing algorithm thus worked well for the extraction of significant HRIs.

4.2. *Feature selection and α optimization*

Feature selection typically resulted in the selection of $\overline{\text{HR}}_{\text{base}}$(selected in 17/17 LOPO CV runs), HR_{peak} (17/17), HR_{start} (17/17) and the pre-ictal SDSD (15/17). The combination of these four features was the most common combination during feature selection (15/17). All these features are easily online extractable with a very limited computational load, making them easier implementable in wearable devices. It took 1785s to analyze 918 h of HR data on a desktop pc with 24 GB RAM and a 3.6 GHz processor using Matlab®.

The α parameter in Eq. (12) was optimized automatically during the training procedure. A value of 2 was chosen the most (12/17 LOPO CV runs), 2.5 was chosen 4 times, 3 only once. If the same α was used for every patient, $\alpha \in [2, 3]$ indeed resulted in the best performance (see Table 3).

All results in this paper are obtained by using a Gaussian kernel $\varphi(.)$ during SVM training. After evaluating the results for the Gaussian kernel, the training of the SVM classifiers was also redone for other kernels using the features mentioned above. No other kernel however led to an increase in performance compared to the Gaussian kernel.

Table 3. Results for fHRI-SVM in case a fixed α is used for all patients during SVM training.

α	1	2	2.5	3	4	5
Se (%)	69.29	81.10	84.25	85.04	85.04	84.25
FP/h	1.32	1.91	2.11	2.26	2.48	2.75

4.3. *Fastened algorithm fHRI-SVM*

A faster seizure detection is possible with a small adjustment to the originally proposed algorithm. As discussed in Sec. 4.2, $\overline{\text{HR}}_{\text{base}}$, pre-ictal SDSD, HR_{start} and HR_{peak} are selected as the used features in 15/17 LOPO CT runs. The first 3 of these features can all be extracted when $\nabla\text{HR}_{\text{max}}$ is found, leading to the possibility to enhance the proposed algorithm. The algorithm can be changed so that once $\nabla\text{HR}_{\text{max}}$ is detected, we assume each new HR measurement HR_k to be the end of the HRI (so that $\text{HR}_{\text{peak}} = \text{HR}_k$). Equations (3a)–(3d) can then already be evaluated, and if this newly formed quadruple of features leads to a seizure HRI (using the original classifier), an alarm can go off much faster. If this does not hold, the procedure keeps iterating until the real end of the HRI is found. This does not lead to many extra false alarms compared to *HRI-SVM* because:

- The filtered HR signal is an increasing signal during the HRI. The parameters evaluated in Eqs. (3a)–(3c) will therefore only increase during the HRI, and so will not cause extra false alarms.
- The parameter in Eq. (3d) can decrease if the HR gradient decreases significantly. This can happen near the end of the HRI as some HR gradients are nearly zero near the end of the HRI for a long period. The impact of this is however limited as it typically only occurs in very strong HRIs that are mainly caused by seizures.
- The used SVM classifier typically led to a classification boundary which could be simplified to

$$\text{class} = \begin{cases} -1 : \text{HR}_{\text{peak}} \leq thr, \\ +1 : \text{HR}_{\text{peak}} > thr, \\ -1 : \text{HR}_{\text{peak}} >= \pm 200 bpm \end{cases}$$

with thr the threshold value as defined by the classification boundary given the other feature values. In this case, no HRIs that were classified as non-seizure in the original algorithm can be classified as a seizure in this approach except if they had a HR_{peak} larger than ±200bpm. Such a high HR is however only reached in this database due to grouped R peak detection errors. This caused some extra false alarms with this adjusted algorithm.

The pseudocode for the fastened version (called fHRI-SVM) is shown in Algorithm 3, which replaces lines 31–40 in Algorithm 2. Unless specifically mentioned, this algorithm and its results are discussed from now on.

4.4. *Results*

Table 4 gives an overview of the obtained results for each patient independently by using the *fHRI-SVM* algorithm. The results of all proposed algorithms and the algorithms from the literature are shown in Table 5. An overall sensitivity of 81.89% (range 50.0–100.0%) is obtained, with on average 1.97 FP/h (range 0.88–3.52FP/h). The seizures were detected on average 17.8s after the seizure onset (range −18.2–54.3s). The used SVM classifier showed a sensitivity of 88.79%, with a specificity of 67.89% in the *HRI-SVM* algorithm.

Algorithm 3 Pseudocode for *fHRI-SVM*.

Input: Online HR data, patient-independent classifier SVM
Output: Information of a significantly strong HRI
1: **for** each HR measurement HR_k at time t_{HR_k} **do**
2: Filter HR data using median filter
3: Compute HR gradient ∇HR_k
4: **if** not currently looking for end of a HRI
5: **if** $\nabla HR_k > 1 bpm/s$
6: Look back for last $\Delta HR \leq 0 bpm/s$: start of HRI t_{start}
7: Extract pre-ictal HR SDSD, $\overline{HR}_{base}$ and HR_{start}
8: Start looking online for t_{end}
9: **end if**
10: **else**
11: Try $t_{end} = t_{HR_k}$ so that $HR_{peak} = HR_k$
12: **if** Eq. 3a-3d apply and SVM(extracted features)=1
13: Significant HRI detected!
14: **end if**
15: **if** real end of HRI is found
16: stop looking for end of HRI
17: **end if**
18: **end if**
19: Check if HR_{rest} needs an update
20: **end for**

Table 4. Results per patient for *fHRI-SVM*.

Patient	Se(%)	FP/h	PPV(%)	$\overline{\text{delay}}$ (s)
1	75.0	1.84	6.52	−16.7
2	80.0	1.14	21.05	17.8
3	100.0	3.52	3.90	9.5
4	61.5	1.72	6.15	54.3
5	60.0	2.96	1.87	32.2
6	80.0	1.58	17.02	9.0
7	100.0	3.21	2.82	4.9
8	90.9	1.91	10.00	12.3
9	100.0	2.71	4.60	18.1
10	100.0	2.37	16.67	−18.2
11	100.0	1.13	10.53	−2.6
12	100.0	2.00	2.31	50.6
13	50.0	2.18	4.00	4.6
14	66.7	0.88	4.76	9.6
15	86.7	2.02	16.15	10.3
16	63.6	1.26	4.67	33.3
17	100.0	1.70	0.44	2.1
Overall	81.89	1.97	5.43	17.8
Pat.-av.	83.20	2.01	7.85	13.6

4.5. *Comparison between HRI-SVM and fHRI-SVM*

By using the *fHRI-SVM* algorithm, the detection delay dropped from 26.54s to 17.83s compared to the original *HRI-SVM* algorithm. Fig. 4 shows the detection delay histograms for both *HRI-SVM* and *fHRI-SVM*. An overall shift towards lower delays can be noticed, causing less large delays (>60s). 83 of the detected seizures (79.8%) were detected within 30s of the seizure onset using *fHRI-SVM*, and 10 seizures (9.6%) were detected before the seizure onset.

The number of false alarms increased slightly to 1.97FP/h using *fHRI-SVM*, but also the sensitivity increased to 81.89%. The slight increase in detections compared to the results of *HRI-SVM* is due to the two possible causes described in Sec. 4.3, which happen only rarely as can be seen in the limited increase in false alarms.

Table 5. Comparison of the results for the different evaluated algorithms. Bold numbers indicate the algorithms with similar sensitivity or FP/h rate as the proposed algorithm.

Method	Overall				Patient-averaged			
	Se (%)	FP/h	PPV (%)	$\overline{\text{delay}}$ (s)	Se (%)	FP/h	PPV (%)	$\overline{\text{delay}}$ (s)
HRI-EXTRACT (Algorithm 1)	91.34	6.00	2.06	25.26	91.73	6.43	2.81	22.08
HRI-SVM (Algorithm 3.5)	**81.10**	**1.93**	5.50	26.54	81.42	1.94	7.98	24.94
fHRI-SVM (Algorithm 3)	**81.89**	**1.97**	5.43	17.83	83.20	2.01	7.85	13.61
De Cooman *et al.*[17]	**81.10**	2.93	3.69	18.28	85.17	3.59	4.77	14.03
Ungureanu *et al.*[12]	55.12	4.56	1.65	19.23	55.51	4.20	5.07	23.33
Osorio(se)[10]	**80.31**	4.19	2.59	15.86	81.88	4.31	3.63	5.89
Osorio(fph)[10]	69.29	**1.98**	4.61	17.07	73.24	2.19	8.49	8.42
vanElmpt(se)[9]	**80.31**	6.69	1.63	10.82	81.66	6.88	3.43	10.63
vanElmpt(fph)[9]	44.88	**2.01**	2.99	16.09	42.42	2.38	6.87	13.71

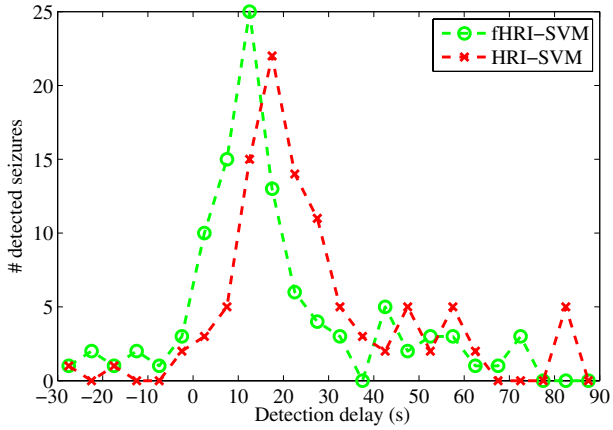

Fig. 4. Histogram of the detection delay between the seizure onset and the alarm time for the proposed seizure detection algorithms.

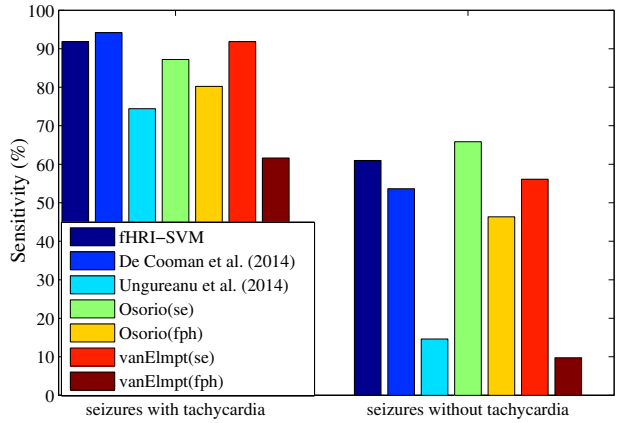

Fig. 5. Sensitivity performance for seizures with and without tachycardia for the different tested algorithms.

4.6. *Comparison between fHRI-SVM and the literature*

The proposed algorithm showed to give the best combination of sensitivity and PPV on the mentioned dataset compared to the tested algorithms of the literature. If around 2FPs/h were requested, this caused a significant sensitivity drop in both Osorio(fph) and vanElmpt(fph). Ungureanu *et al.* resulted in both significant lower sensitivity and PPV compared to the proposed algorithm. The main reason for this is that this algorithm is focused on detecting seizures with high HR values ($>$ 110bpm), and showed problems in the detection of seizures that did not lead to tachycardia (defined here as $\text{HR}_{\text{peak}} > 100$bpm and $\Delta\text{HR} > 10$bpm). This is illustrated in Fig. 5, which shows the sensitivity of all algorithms for both seizures leading to tachycardia (86/127 seizures) or not (41/127 seizures). All algorithms were able to detect at least 60% of the seizures with tachycardia, but bigger differences were found for the nontachycardia seizures. The drop in sensitivity for the fph-based versions compared to the se-based versions of Osorio and vanElmpt were mainly caused by a big drop in sensitivity for the nontachycardia seizures. The proposed method was able to detect 91.9% of the tachycardia seizures and 61.0% of the nontachycardia seizures.

Figure 6(a) shows the boxplots for the inter-patient sensitivity variability for the different tested algorithms. The proposed algorithm always led to a sensitivity of at least 50%. All other algorithms from literature showed a greater sensitivity variability, leading to 0% sensitivity for some patients in Ref. 12 and vanElmpt(fph).

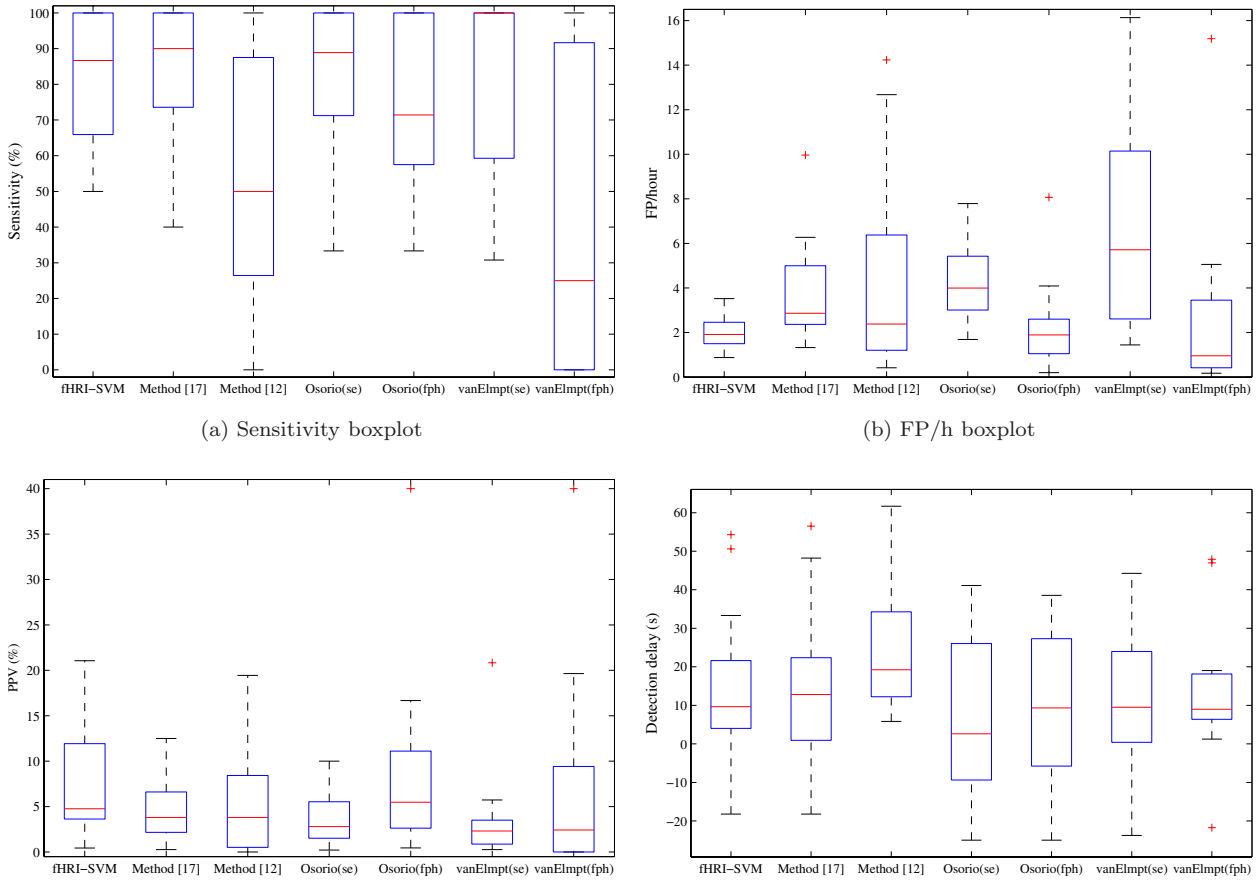

(a) Sensitivity boxplot

(b) FP/h boxplot

(c) PPV boxplot

(d) Detection delay boxplot

Fig. 6. Boxplots showing the inter-patient variability in sensitivity (a), FP/h (b), PPV (c) and detection delay (d) for the different tested algorithms.

Bigger differences were found in the number of false positives when comparing the proposed algorithm to the tested algorithms from the literature. The proposed method led towards at least 2.2 FP/h less than the other algorithms with comparable sensitivity, a decrease of at least 50% of false alarms. Figure 6(b) shows that the proposed method also resulted in less inter-patient variability in the number of false alarms. The proposed algorithm thus not only worked best overall for these statistics, but it also resulted in the least inter-patient variability for both FP/h and sensitivity, leading to reasonable results for all patients. PPV values (see Fig. 6(c)) vary more between patients for all algorithms, but this will be discussed in Sec. 4.7. Figure 7 shows the results for all evaluation measurements per patient for all tested algorithms.

Figure 8 shows the sensitivity and FP/h performance for the fHRI-SVM algorithm and the algorithm from Ref. 17 in case the SVM bias term b is altered. Also the results for different parameter values for the algorithms from Refs. 10 and 9 on this dataset are shown. It can be seen that the fHRI-SVM algorithm always led to the best sensitivity-FP/h combination (if Se>50%). Some possible explanations why these algorithms from the literature show significantly lower results on this dataset, as discussed in the corresponding papers, are:

- A much larger patient group has been analyzed than in Refs. 9 (3 patients) and 12 (5 patients).
- Both day and night data were used, while Ref. 12 only discussed detection during the night.
- No preselection on the patients is done based on their ictal HR or motoric responses, nor on their seizure frequency.[9,12] Only a preselection towards TLE patients is done in this paper, which contained a wide range of seizures and is

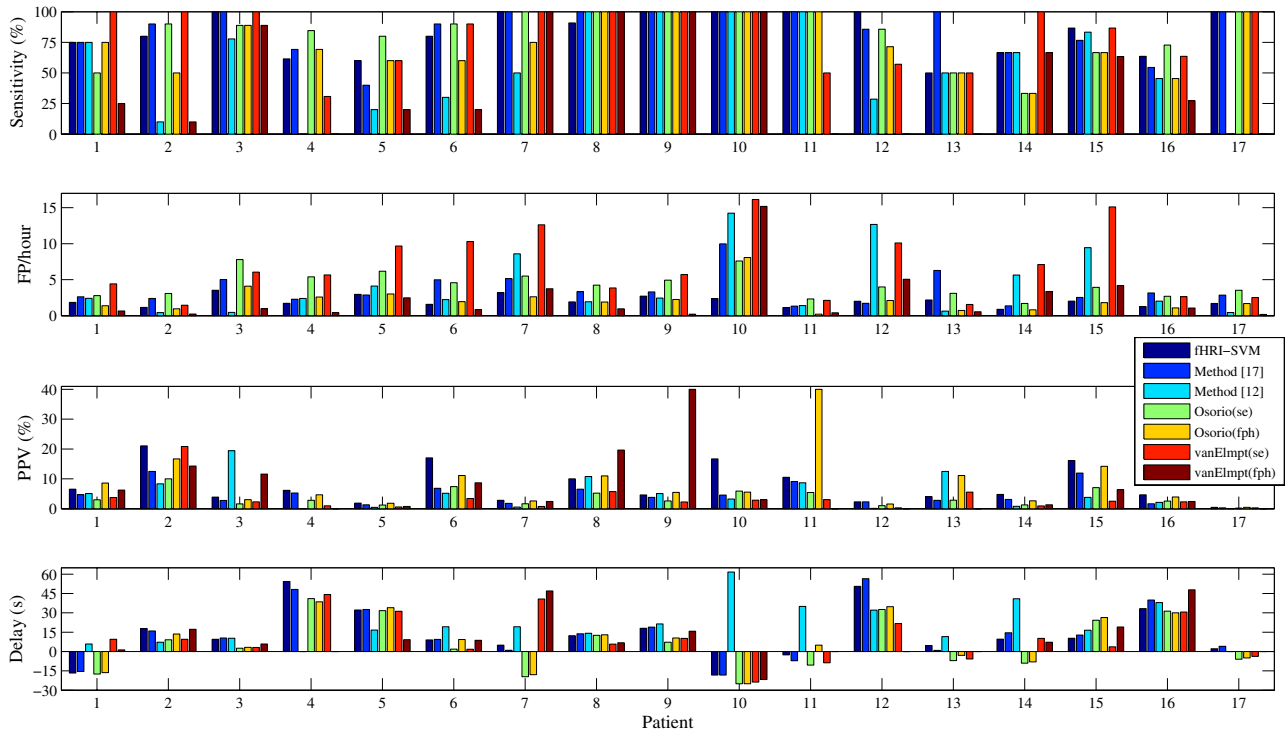

Fig. 7. Patient-specific sensitivity, FP/h, PPV and detection delay results for the different tested patient-independent seizure detection algorithms.

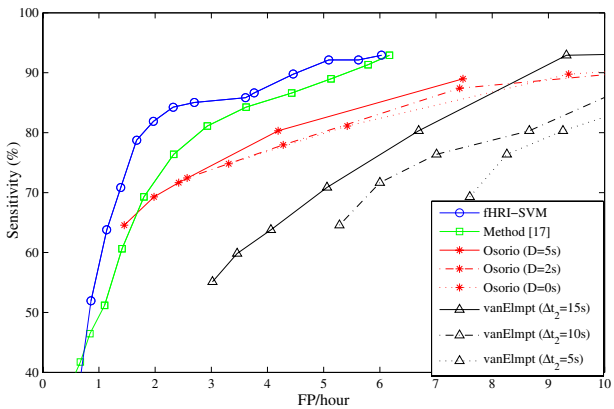

Fig. 8. Sensitivity versus FP/h results for the different tested algorithms. For fHRI-SVM and the method from Ref. 17 the different performance results were found by altering the SVM bias term b. For the Osorio and vanElmpt algorithm, the parameter values from the papers are altered. For Osorio, each line contains a constant delay term D with varying heart rate threshold values.[10] For vanElmpt, each line contains a constant second time window Δt_2, with changing heart rate threshold values.[9] We refer to the corresponding papers for details of these algorithms and their parameters.

the largest group of epilepsy patients. Sensitivity results of Ref. 10 were only computed on clinical seizures.

- No restriction was done on the patient movements[10] (although they are still limited to the hospital rooms).
- No manual correction of R peak detection errors was performed.[9]

When looking at the detection delay, the *HRI-SVM* algorithm detected the seizures (much) later than the other algorithms (see Table 5). *HRI-SVM* detected the seizures on patient-average after 24.9s, while for Osorio(se) this was on average 5.9s after the seizure onset. The main reason for this, is the fact that *HRI-SVM* is required to wait for the HRI to stop, whereas other algorithms can already trigger an alarm sooner. It seems however that detecting the seizures too soon also causes a large amount of extra false alarms. Figure 9 illustrates this for a nonseizure and a seizure HRI coming from the same patient during sleep. The start of both HRIs are similar, hence making it hard to detect this seizure very rapidly

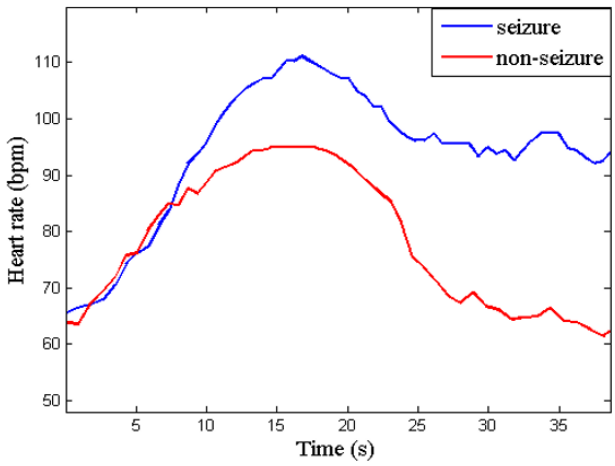

Fig. 9. Comparison of a seizure and a nonseizure HRI originating from the same patient. Both HRIs were detected during sleep, within only a few hours of each other.

without detecting the nonseizure HRI. The only difference seems to be that the seizure HRI maintains the strong HR acceleration longer, thus leading to a higher peak HR. *fHRI-SVM* tries to alarm as soon as it is sufficiently sure that the HRI is caused by a seizure. More than 50% less false alarms were found compared to the literature in this way, with only a limited extra patient-averaged detection delay (3.0s patient-averaged compared to vanElmpt(se), 7.7s compared to Osorio(se)). Part of this extra delay (typical 3–5s) is caused by the median filter in *HRI-EXTRACT*. The results however show that this step is very helpful in removing R peak detection errors from the heart rate signal, hence getting more robust seizure detection results.

4.7. *Inter-patient variability*

As the results vary strongly for different patients (see Fig. 6 and 7), a closer look is taken on the inter-patient variability for the sensitivity, PPV, FP/h and detection delay using the *fHRI-SVM* algorithm.

4.7.1. *Sensitivity*

Only two patients did not have a sensitivity higher than 60%. For patient 5, only 3/5 seizures were detected, as the other two seizures did not contain strong ictal HRIs (ΔHR = 20bpm with Δt_{HRI} = 80s).

Patient 13 only showed 50% accuracy as one of the two seizures was missed due to a high pre-ictal HR $\mathrm{HR}_{\mathrm{base}}$. Seizures in other patients were typically missed by atypical HRIs for that patient or due to strong ictal ECG noise.

4.7.2. *FP/h*

The number of FP/h depended mainly on how often each patient had nonepileptic sympathetic activations during the recordings and how strong these sympathetic activations typically were. For patients for which these were typically stronger (such as children), nonepileptic sympathetic HRIs (caused by f.e. arousals or mental stress) led much faster to stronger ΔHR values, causing more FPs. In some patients, the average ECG noise levels (both ictal and inter-ictal) were much higher compared to other patients. This unavoidably led to R peak detection errors and extra false alarms. Although the effect was rather limited for the proposed algorithm, this led to a much higher FP/h rate for example patient 10 for the algorithms from the literature (see Fig. 7).

4.7.3. *PPV*

As described above, the number of FPs mainly depended on the number of nonepileptic sympathetic HRIs, and was independent on the number of seizures. The PPV values were therefore strongly correlated with the seizure frequency. Big negative outliers in PPV values were found in patients with a low seizure frequency (see e.g. patient 17).

4.7.4. *Detection delay*

The found detection delay for *fHRI-SVM* mainly depended on two factors:

- The start of the HRI compared to the EEG onset: Previous studies showed that the time difference between the HR changes and the EEG onset can vary between different seizures.[8,29] HRIs can start either just before or after the EEG onset. The sooner the HRI starts, the higher the chance to detect the seizure faster.
- The strength of the sympathetic activation: The seizure can only be detected when the HR has increased sufficiently compared to $\overline{\mathrm{HR}}_{\mathrm{base}}$. For patients with relative slowly increasing sympathetic activations, it took longer to get to this temporary $\mathrm{HR}_{\mathrm{peak}}$ required for alarming (see for example patients 4 and 12).

4.8. *Relationship between clinical phenomena and seizure detection results*

For home monitoring applications, it is interesting to see how the different algorithms cope with different types of ictal motoric manifestations. The seizures are therefore divided into three categories:

- Class 1 (27 seizures): Nonmotor seizures with no clear motoric manifestations (except for eye-blinking and lip movements).
- Class 2 (45 seizures): Seizures with discrete motoric manifestations (subtle dystonia and discrete motoric agitation).
- Class 3 (55 seizures): Strong convulsive seizures including tonic, clonic and tonic-clonic seizures.

Table 1 gives an overview of which seizure classes were found in each patient. The seizures from group 3 are clinically the most severe seizures, which most alarm systems aim to detect due to their high risk of injuries.[5] Patients can however lose their consciousness during most of the class 1 seizures, which might indirectly lead to potential dangerous situations (e.g. walking on stairs), so it is also important to detect those seizures. Fig. 10 shows the sensitivity for each class of seizures for the evaluated seizure detection algorithms. It can be seen that for most algorithms, the sensitivity is higher for seizures with ictal motoric activity (classes 2 and 3) than for nonmotor seizures. The main reason for this is the fact that these nonmotor seizures have a much lower tachycardia occurrence (37.0%) compared to classes 2 and 3 (68.9% and 81.8%), making it harder to detect them. Class 2 seizures are found slightly easier by methods from literature than class 3 seizures, which is probably due to the fact that these contain less ECG noise due to more subtle ictal movements. The proposed method was able to detect 74.0%, 82.2% and 85.5% of the seizures from respectively classes 1, 2 and 3.

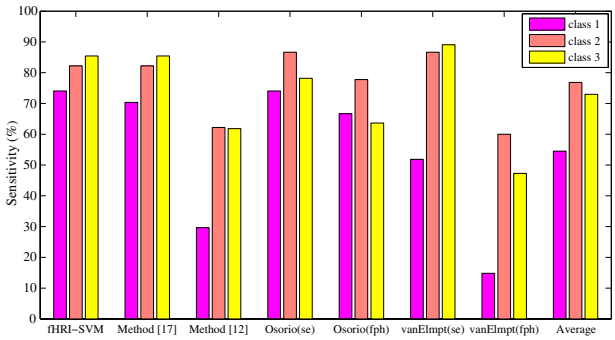

Fig. 10. Sensitivity results for each class of seizure severity for the different tested algorithms. The average sensitivity over all algorithms for the three severity classes is also shown in this figure.

4.9. *Applications of HR-based seizure detection*

Automated seizure detection algorithms using ECG can be used for several purposes. A first purpose is as part of an alarm system in a home environment. The algorithm can automatically give a warning to caregivers whenever a seizure is detected by the algorithm. This is a useful system, certainly for children with epilepsy and their parents. The number of FP/h for these patient-independent algorithms show that work still needs to be done in order to make such a system successful for 24/7 monitoring. The number of FPs during the day are typically too high due to patient activity. A previous study on children with epilepsy showed that such a system can however produce better FP rates ($\pm$1FP/h) when the system is used during the night.[14] In this case, the false alarm rate mainly depends on the sleep quality of the patient. These results could however not be replicated here due to the use of sleep deprivation during monitoring.

A second practical use would be to include such an automated seizure detection in a closed-loop VNS system. VNS is shown to be effective for preventing and possibly shortening ongoing seizures.[3] By automatically detecting the seizures, it can trigger the VNS activation during this seizure. It is important to keep the number of false VNS activations to a minimum to prolong the battery life-time. The proposed method showed a strong decrease in false alarms for a similar sensitivity compared to the literature, hence avoiding false VNS activations. Due to the slightly increased detection delay, it will however take a few seconds longer to stop ongoing seizures.

The system can also be used in the hospitals or revalidation centers. For the investigated seizures from TLE patients, over 90% of the seizures were accompanied with an ictal strong HRI. An interesting fact can be seen for the patients in which the seizures were not (clearly) visible in EEG. Automated seizure detection algorithms using the EEG

would probably not be able to detect these seizures accurately, whereas the proposed algorithm using ECG was able to correctly detect 83.87% of these seizures (31 seizures in total). This algorithm can thus also be useful in the epilepsy monitoring facilities, possibly as enhancement of online seizure detection applications using EEG.[30–32] The discussed methods also have the advantage that some of the seizures can be detected by using ECG before the seizure is clearly visible during video-EEG monitoring (as can be seen for example in Fig. 4).

Due to the use of a patient-independent algorithm, the applications can be used from the beginning, without requiring patient-specific data. This approach makes the algorithm more useful for short-term applications, or for the start of long-term applications such as the alarm system or an automated seizure diary. It does not require manual analysis of the patient's data, and no manual setting of parameters should be done.

4.10. *Remaining issues*

The downside of the approach is however that on a longer time-scale, patient-specific algorithms will obviously lead to a better performance. Both approaches can however be combined. A possible solution would be to start from a patient-independent algorithm, which can learn the patient-specific characteristics on-the-run (using adaptive learning) when more patient-specific data becomes available. This way, the algorithm will converge to a patient-specific algorithm over time.[13] This is one of the foci for future investigation.

Another option to improve the performance for patient-independent algorithms, would be to add extra modalities to the system. Modalities such as accelerometry, electromyogram and electrical dermal activity have shown to be useful for detecting seizures including movements.[25,33–36] Also using ECG morphology features and cardiorespiratory dynamics could possibly enhance the performance.[37]

A crucial problem for automated seizure detection using ECG, remains the high noise levels in the ECG. Although an R peak detection algorithm was used that showed similar performance as online state-of-the-art algorithms, still a lot of R peak detections errors were found, both ictal and interictal. These obviously influence the performance of the detector, and cause a significant part of the missed seizures and false alarms,[13] but seems to be unavoidable when acquiring the ECG for every day use. The proposed method tried to cope with it by using the median filter on the tachogram, which filtered out a lot of noisy HR measurements, but also included an extra detection delay to the system (typically ±3–5s).

5. Conclusion

A patient-independent online algorithm using only ECG was proposed for the automated detection of complex partial and secondary generalized seizures. The method showed a significant performance increase in sensitivity and PPV compared to other patient-independent methods from the literature, but also resulted in a slightly larger detection delay. The selected features from feature extraction showed that the required features are easy to compute in an online fashion and make the proposed algorithm implementable for wearable devices. Future work will go into improving the performance by adding information from accelerometry and electromyogram to the system for the detection of strong convulsive seizures.

Acknowledgments

Research supported by Bijzonder Onderzoeksfonds KU Leuven (BOF): Center of Excellence (CoE): PFV/10/002(OPTEC), SPARKLE #: IDO-13-0358, C24/15/036, C32/16/00364; Fonds voor Wetenschappelijk Onderzoek-Vlaanderen (FWO): G.0A55.13N (Deep brain stimulation); Agentschap Innoveren & Ondernemen (VLAIO): STW 150466 OSA +, O&O HBC 2016 0184 eWatch; iMinds Medical Information Technologies: ICON: HBC.2016.0167 SeizeIT; Belgian Federal Science Policy Office IUAP #P7/19/ (DYSCO, 'Dynamical systems, control and optimization', 2012–2017); Belgian Foreign Affairs-Development Cooperation VLIR UOS programs (2013–2019); EU: European Union's Seventh Framework Programme (FP7/2007–2013): EU MC ITN TRANSACT 2012: #316679, The HIP Trial: #260777; Erasmus +: INGDIVS 2016-1-SE01-KA203-022114; European Research Council: The research leading to these results has received funding from the European Research Council under the European Union's Seventh Framework

Programme (FP7/2007–2013)/ERC Advanced Grant: BIOTENSORS (n^o 339804). This paper reflects only the authors' views and the Union is not liable for any use that may be made of the contained information. Thomas De Cooman is supported by an IWT SBO PhD grant.

References

1. D. Hirtz, D. Thurman, K. Gwinn-Hardy, M. Mohamed, A. Chaudhuri and R. Zalutsky, How common are the common neurologic disorders? *Neurology* **68**(5) (2007) 326–337.
2. K. Vonck and P. Boon, Epilepsy: Closing the loop for patients with epilepsy, *Nat. Rev. Neurol.* **11**(5) (2015) 252–254.
3. K. G. Hampel, H. Vatter, C. E. Elger and R. Surges, Cardiac-based vagus nerve stimulation reduced seizure duration in a patient with refractory epilepsy, *Seizure* **26** (2015) 81–85.
4. A. Schulze-Bonhage, F. Sales, K. Wagner, R. Teotonio, A. Carius, A. Schelle and M. Ihle, Views of patients with epilepsy on seizure prediction devices, *Epilepsy Behavior* **18**(4) (2010) 388–396.
5. A. Van de Vel, K. Cuppens, B. Bonroy, M. Milosevic, K. Jansen, S. Van Huffel, B. Vanrumste, L. Lagae and B. Ceulemans, Non-eeg seizure-detection systems and potential sudep prevention: State of the art, *Seizure* **22**(5) (2013) 345–355.
6. K. Jansen and L. Lagae, Cardiac changes in epilepsy, *Seizure* **19**(8) (2010) 455–460.
7. M. Zijlmans, D. Flanagan and J. Gotman, Heart rate changes and ECG abnormalities during epileptic seizures: Prevalence and definition of an objective clinical sign, *Epilepsia* **43**(8) (2002) 847–854.
8. F. Leutmezer, C. Schernthaner, S. Lurger, K. Pötzelberger and C. Baumgartner, Electrocardiographic changes at the onset of epileptic seizures, *Epilepsia* **44**(3) (2003) 348–354.
9. W. van Elmpt, J. Wouter, T. Nijsen, P. Griep and J. Arends, A model of heart rate changes to detect seizures in severe epilepsy, *Seizure* **15**(6) (2006) 366–375.
10. I. Osorio, Automated seizure detection using EKG, *Int. J. Neural Syst.* **24**(2) (2014) 1450001.
11. F. Massé, M. Van Bussel, A. Serteyn, J. Arends and J. Penders, Miniaturized wireless ECG monitor for real-time detection of epileptic seizures, *ACM Trans. Embedded Comput. Syst.* **12**(4) (2013) 102.
12. C. Ungureanu, V. Bui, W. Roosmalen, R. M. Aarts, J. B. Arends, R. Verhoeven and J. J. Lukkien *et al.*, A wearable monitoring system for nocturnal epileptic seizures, *2014 8th Int. Symp. Medical Information and Communication Technology* (*ISMICT*) (IEEE, 2014), pp. 1–5.
13. T. De Cooman, A. Van de Vel, B. Ceulemans, L. Lagae, B. Vanrumste and S. Van Huffel, Online detection of tonic-clonic seizures in pediatric patients using ECG and low-complexity incremental novelty detection, in *Proc. 37th Annual Int. Conf. IEEE Engineering in Medicine and Biology Society* (*EMBC2015*) (IEEE, 2015), pp. 5597–5600.
14. T. De Cooman, A. Van de Vel, B. Ceulemans, L. Lagae, W. Van Paesschen, B. Vanrumste and S. Van Huffel, Estimation of the maximal heart rate to improve online tonic-clonic seizure detection using ECG, *Computing in Cardiology Conference* (*CinC*), *2015* (IEEE, 2015), pp. 977–980.
15. B. R. Greene, P. De Chazal, G. B. Boylan, S. Connolly and R. B. Reilly, Electrocardiogram based neonatal seizure detection, *IEEE Trans. Biomed. Eng.* **54**(4) (2007) 673–682.
16. O. Doyle, A. Temko, W. Marnane, G. Lightbody and G. Boylan, Heart rate based automatic seizure detection in the newborn, *Medi. Eng. Phys.* **32**(8) (2010) 829–839.
17. T. De Cooman, E. Carrette, P. Boon, A. Meurs and S. Van Huffel, Online seizure detection in adults with temporal lobe epilepsy using single-lead ECG, in *Proc. 22nd European Signal Processing Conf.* (*EUSIPCO*), *2014* (IEEE, 2014), pp. 1532–1536.
18. Y.-C. Yeh and W.-J. Wang, QRS complexes detection for ECG signal: The difference operation method, *Comput. Methods Prog. Biomed.* **91**(3) (2008) 245–254.
19. G. B. Moody and R. G. Mark, The impact of the mit-bih arrhythmia database, *IEEE Eng. Med. Biol. Mag.* **20**(3) (2001) 45–50.
20. A. L. Goldberger, L. A. Amaral, L. Glass, J. M. Hausdorff, P. C. Ivanov, R. G. Mark, J. E. Mietus, G. B. Moody, C.-K. Peng and H. E. Stanley, Physiobank, physiotoolkit, and physionet components of a new research resource for complex physiologic signals, *Circulation* **101**(23) (2000) e215–e220.
21. J. Pan and W. J. Tompkins, A real-time qrs detection algorithm, *IEEE Trans. Biomed. Eng.* **3** (1985) 230–236.
22. P. Smith, S. Howell, L. Owen and L. Blumhardt, Profiles of instant heart rate during partial seizures, *Electroencephalogr. Clin. Neurophysiol* **72**(3) (1989) 207–217.
23. J. Jeppesen, S. Beniczky, A. Fuglsang-Frederiksen, P. Sidenius and Y. Jasemian, Detection of epileptic-seizures by means of power spectrum analysis of heart rate variability: A pilot study, *Technol. Health Care* **18**(6) (2010) 417–426.
24. A. Camm, M. Malik, J. Bigger, G. Breithardt, S. Cerutti, R. Cohen, P. Coumel, E. Fallen, H. Kennedy, R. Kleiger *et al.*, Heart rate variability: standards of measurement, physiological interpretation and clinical use. Task force of the european society of cardiology and the north american society of pacing and electrophysiology, *Circulation* **93**(5) (1996) 1043–1065.

25. M. Milosevic, A. Van de Vel, B. Bonroy, B. Ceulemans, L. Lagae, B. VanRumste and S. Van Huffel, Automated detection of tonic-clonic seizures using 3d accelerometry and surface electromyography in pediatric patients, *Biomed. Health Inform. IEEE J.* (2015).
26. V. Vapnik, *The Nature of Statistical Learning Theory* (Springer Science & Business Media, 1999).
27. R. Akbani, S. Kwek and N. Japkowicz, Applying support vector machines to imbalanced datasets, in *Machine Learning: ECML 2004* (Springer, 2004), pp. 39–50.
28. M. Hirsch, D.-M. Altenmller and A. Schulze-Bonhage, Latencies from intracranial seizure onset to ictal tachycardia: A comparison to surface eeg patterns and other clinical signs, *Epilepsia* **10** (2015) 1639–1647.
29. G. Di Gennaro, P. P. Quarato, F. Sebastiano, V. Esposito, P. Onorati, L. G. Grammaldo, G. N. Meldolesi, A. Mascia, C. Falco, C. Scoppetta *et al.*, Ictal heart rate increase precedes EEG discharge in drug-resistant mesial temporal lobe seizures, *Clinical Neurophysiol.* **115**(5) (2004) 1169–1177.
30. A. T. Tzallas, D. G. Tsalikakis, E. C. Karvounis, L. Astrakas, M. Tzaphlidou, M. G. Tsipouras and S. Konitsiotis, *Automated Epileptic Seizure Detection Methods: A Review Study* (INTECH Open Access Publisher, 2012).
31. H. Adeli and S. Ghosh-Dastidar, *Automated EEG-based Diagnosis of Neurological Disorders: Inventing the Future of Neurology* (CRC Press, 2010).
32. S. Ghosh-Dastidar, H. Adeli and N. Dadmehr, Principal component analysis-enhanced cosine radial basis function neural network for robust epilepsy and seizure detection, *IEEE Trans. Biomed. Eng.* **55**(2) (2008) 512–518.
33. K. Cuppens, P. Karsmakers, A. Van de Vel, B. Bonroy, M. Milosevic, S. Luca, T. Croonenborghs, B. Ceulemans, L. Lagae, S. Van Huffel *et al.*, Accelerometry-based home monitoring for detection of nocturnal hypermotor seizures based on novelty detection, *IEEE J. Biomed. Health Inform.* **18**(3) (2014) 1026–1033.
34. S. Beniczky, T. Polster, T. W. Kjaer and H. Hjalgrim, Detection of generalized tonic–clonic seizures by a wireless wrist accelerometer: A prospective, multicenter study, *Epilepsia* **54**(4) (2013) e58–e61.
35. I. Conradsen, S. Beniczky, K. Hoppe, P. Wolf and H. B. Sorensen, Automated algorithm for generalized tonic–clonic epileptic seizure onset detection based on semg zero-crossing rate, *IEEE Trans. Biomed. Eng.* **59**(2) (2012) 579–585.
36. M.-Z. Poh, T. Loddenkemper, C. Reinsberger, N. C. Swenson, S. Goyal, M. C. Sabtala, J. R. Madsen and R. W. Picard, Convulsive seizure detection using a wrist-worn electrodermal activity and accelerometry biosensor, *Epilepsia* **53**(5) (2012) e93–e97.
37. C. Varon, K. Jansen, L. Lagae and S. Van Huffel, Can ECG monitoring identify seizures? *J. Electrocardiol.* **48**(6) (2015) 1069–1074.